

A Narrow Band-Based Multiscale Multigroup Full-Spectrum k -Distribution Method for Radiative Transfer in Nonhomogeneous Gas-Soot Mixtures

Gopalendu Pal
Michael F. Modest¹

Fellow ASME
e-mail: mfmodest@psu.edu

Department of Mechanical and Nuclear
Engineering,
Pennsylvania State University,
University Park, PA 16802

The full-spectrum k -distribution (FSK) approach has become a promising method for radiative heat transfer calculations in strongly nongray participating media, due to its ability to achieve high accuracy at a tiny fraction of the line-by-line (LBL) computational cost. However, inhomogeneities in temperature, total pressure, and component mole fractions severely challenge the accuracy of the FSK approach. The objective of this paper is to develop a narrow band-based hybrid FSK model that is accurate for radiation calculations in combustion systems containing both molecular gases and nongray particles such as soot with strong temperature and mole fraction inhomogeneities. This method combines the advantages of the multigroup FSK method for temperature inhomogeneities in a single species, and the modified multiscale FSK method for concentration inhomogeneities in gas-soot mixtures. In this new method, each species is considered as one scale; the absorption coefficients within each narrow band of every gas scale are divided into M exclusive spectral groups, depending on their temperature dependence. Accurate and compact narrow band multigroup databases are constructed for combustion gases such as CO_2 and H_2O . Sample calculations are performed for a 1D medium and also for a 2D axisymmetric combustion flame. The narrow band-based hybrid method is observed to accurately predict heat transfer from extremely inhomogeneous gas-soot mixtures with/without wall emission, yielding close-to-LBL accuracy. [DOI: 10.1115/1.4000236]

1 Introduction

Radiative heat transfer is a very important mode of heat transfer in high temperature combustion systems and atmospheric processes. Radiation calculations in participating media can be most accurately performed by the line-by-line (LBL) approach. However, LBL calculations require huge computer resources (both computational time and memory). For accurate and computationally efficient solutions of the radiative transfer equation (RTE), several models have been proposed, applying the concept of reordering the absorption coefficient across the entire spectrum. These include the spectral-line-based weighted-sum-of-gray-gases (SLW) model [1], the absorption distribution function (ADF) method [2], and the full-spectrum k -distribution (FSK) method [3]. Although the FSK scheme is exact for radiative calculations in homogeneous media, its application to strongly inhomogeneous emitting-absorbing mixtures, containing both molecular gases and nongray soot particles, challenges its accuracy.

Several advancements to the k -distribution method have been proposed to address the shortcomings of the basic FSK scheme. The advanced k -distribution methods with their advantages and shortcomings are summarized as follows.

- *Single scale FSK*. 8–10 RTEs. Advantages: Most CPU efficient; accurate for moderately inhomogeneous media. Dis-

advantages: Inaccurate for strongly inhomogeneous media; problems with mixing of species [3].

- *Narrow band-based single-scale FSK*. 8–10 RTEs. Advantages: Most CPU efficient; mixing of multiphase species; accurate for moderately inhomogeneous media. Disadvantages: Inaccurate for strongly inhomogeneous media [4].
- *Fictitious gas*. $(8-10)^N$ RTEs. Advantages: Accurate for mixing (gas only) temperature and species inhomogeneity. Disadvantages: Inaccurate for multiphase mixing; computationally expensive [2].
- *Multiscale FSK (MSFSK)*. $N \times (8-10)$ RTEs. Advantages: Accurate for mixing and species (gas only) inhomogeneity. Disadvantages: Inaccurate for strong temperature inhomogeneity and multiphase mixing [5].
- *Multigroup FSK (MGFSK)*. $M \times (8-10)$ RTEs. Advantages: Accurate for temperature inhomogeneity in a single gas. Disadvantages: No mixing of species; inaccurate for species inhomogeneity [6].
- *Narrow band-based MSFSK*. $N \times (8-10)$ RTEs. Advantages: Better accuracy for mixing of gases than MSFSK; potential for multiphase mixing. Disadvantages: Inaccurate for strong temperature inhomogeneity [7].
- *Multiscale multigroup FSK (MSMGFSK)*. $N \times M \times (8-10)$ RTEs. Advantages: Accurate for general inhomogeneity problems in gas mixtures. Disadvantages: Inaccurate for multiphase mixing [8].
- *Narrow band-based modified MSFSK*. $N \times (8-10)$ RTEs. Advantages: Accurate for multiphase mixing and species in-

¹Corresponding author.

Contributed by the Heat Transfer Division of ASME for publication in the JOURNAL OF HEAT TRANSFER. Manuscript received November 26, 2008; final manuscript revised April 10, 2009; published online December 9, 2009. Assoc. Editor: Yogesh Jaluria.

homogeneity. Disadvantages: Inaccurate for strong temperature inhomogeneity [9].

Soot radiation constitutes an important part of radiation calculations in luminous flames. Because of the difficulties in soot modeling, soot radiation in combustion flames was commonly treated as gray [10]. Nongray soot with gas mixtures was investigated by Solovjov and Webb [11] using the SLW method, by Wang et al. [12] using the single-scale FSK method, and by Pal and Modest [9] using the narrow band-based modified MSFSK method. The modified MSFSK method has been found to produce high accuracy for isothermal multiphase mixtures with species concentration inhomogeneities. However, the modified MSFSK method fails in the presence of strong temperature inhomogeneities.

FSK calculations are very accurate and time efficient, provided that the required full-spectrum k -distributions are known, which are tedious to compile from spectroscopic databases. Wang and Modest [13] compiled a high accuracy, compact database of narrow band k -distributions for CO_2 and H_2O . Full-spectrum multigroup databases (with 32 groups for each species) were constructed by Zhang and Modest [6] for carbon dioxide and water vapor. It has been reported that close-to-LBL accuracy can be achieved by considering only four such groups. Recently, Pal and Modest [9] constructed a more accurate and compact full-spectrum multigroup database containing four groups for each species with spectral absorption coefficients for water vapor calculated from HITEMP 2000, and for carbon dioxide from CDS-1000, which is considered more reliable [8]. The full-spectrum multigroup databases can be used for nonhomogeneous mixtures of gases only. Hence, narrow band multigroup databases are needed for the important combustion gases for accurate mixing of gases and nongray soot at the narrow band level.

In the present work, we have extended the previous (full-spectrum-based) hybrid MSMGFSK method to a narrow band-based hybrid MSMGFSK method, to allow incorporation of nongray soot into the gas mixture. In this method, soot is treated as a single-group scale, while the combustion gases, such as CO_2 and H_2O , can have a maximum of four scalable groups each. An accurate and compact narrow band multigroup database has been constructed by grouping the absorption coefficients within each narrow band of CO_2 and H_2O into four groups, with absorption coefficients of H_2O calculated from HITEMP 2000, and for CO_2 from CDS-1000. Wall emission is treated within the soot scale as was done in the modified MSFSK method [9]. First, a brief mathematical discussion of the narrow band-based MSMGFSK method is presented here, followed by a discussion of the construction of the narrow band multigroup database. Sample calculations are performed for a 1D medium with step changes in species concentration and temperature with/without wall emission, and also for a 2D axisymmetric jet flame. For all cases, results are compared with FSK, MSFSK, and LBL calculations.

2 The Narrow Band-Based MSMGFSK Approach

A brief mathematical derivation of the narrow band-based MSMGFSK method is presented here. A participating medium containing molecular gases and nongray soot is considered. Scattering from the medium is assumed to be gray. The radiative transfer equation (RTE) for such a medium can be written as [14]

$$\frac{dI_\eta}{ds} = \kappa_\eta(\underline{\phi})I_{b\eta} - (\kappa_\eta(\underline{\phi}) + \sigma_s)I_\eta + \frac{\sigma_s}{4\pi} \int_{4\pi} I_\eta(\hat{s}')\Phi(\hat{s}, \hat{s}')d\Omega' \quad (1)$$

which is subject to the boundary condition

$$\text{at } s=0: \quad I_\eta = \epsilon I_{b\eta} + \frac{1-\epsilon}{\pi} \int_{2\pi} I_\eta \hat{n} \cdot \hat{s} d\Omega \quad (2)$$

Here, I_η is the spectral radiative intensity, κ_η is the absorption coefficient, $I_{b\eta}$ is the spectral blackbody intensity (or Planck function), σ_s is the gray scattering coefficient, Φ is the scattering phase function, and wavenumber η is the spectral variable. The vector $\underline{\phi}$ contains state variables that affect κ_η , which include temperature T , total pressure P , and gas mole fractions x : $\underline{\phi} = (P, T, x)$. The boundary wall has been assumed to be gray and diffuse with ϵ being the emittance, \hat{n} being the surface normal, \hat{s} being the unit direction vector of incoming ray radiation, and Ω being the solid angle.

The mixture's spectral absorption coefficient κ_η is first separated into contributions from $N-1$ component gases and soot, and the radiative intensity I_η is also broken up accordingly

$$\kappa_\eta = \sum_{n=1}^N \kappa_{n\eta} \quad I_\eta = \sum_{n=1}^N I_{n\eta} \quad (3)$$

The RTE in Eq. (1) is transformed into N component RTEs, one for each species or scale. For each scale, this leads to

$$\frac{dI_{n\eta}}{ds} = \kappa_{n\eta}(\underline{\phi})I_{b\eta} - (\kappa_\eta(\underline{\phi}) + \sigma_s)I_{n\eta} + \frac{\sigma_s}{4\pi} \int_{4\pi} I_{n\eta}(\hat{s}')\Phi(\hat{s}, \hat{s}')d\Omega', \quad \text{for } n=1, \dots, N \quad (4)$$

The intensity $I_{n\eta}$ is due to the emission by the n -th scale, but subject to absorption by all the scales. Now the spectral locations of the n -th gas absorption coefficients $\kappa_{n\eta}$ along with the n -th gas scale's radiative intensity $I_{n\eta}$ are sorted into M exclusive groups, that is

$$\kappa_{n\eta} = \sum_{m=1}^{M_n} \kappa_{nm\eta} \quad I_{n\eta} = \sum_{m=1}^{M_n} I_{nm\eta} \quad \text{for } n=1, \dots, N-1 \quad (5)$$

Considering the soot scale as a single-group scale, the RTE for the m -th group of the n -th gas scale is transformed into

$$\frac{dI_{nm\eta}}{ds} = \kappa_{nm\eta}(\underline{\phi})I_{b\eta} - (\kappa_\eta(\underline{\phi}) + \sigma_s)I_{nm\eta} + \frac{\sigma_s}{4\pi} \int_{4\pi} I_{nm\eta}(\hat{s}')\Phi(\hat{s}, \hat{s}')d\Omega', \quad \text{for } n=1, \dots, N-1; \quad m=1, \dots, M_n(\text{gas scales}) \quad (6)$$

Note that the intensity $I_{nm\eta}$ is due to the emission by the m -th group of the n -th gas species (the nm -th group), but subject to absorption by all groups of the other gases, soot (single-group scale), and its own group. There is no overlap among groups of a single species and, therefore, there is no emission over wavenumbers where $\kappa_{nq\eta}(q \neq m)$ absorbs. Thus, in Eq. (6)

$$\kappa_\eta = \kappa_{nm\eta} + \sum_{l=1}^N \sum_{q=1}^{M_l} \kappa_{lq\eta} \quad (7)$$

As was done in the modified MSFSK formulations [9], radiation from soot and from wall emission are combined into a single scale, due to their continuous nature. When wall emissions is added to the soot scale, Eq. (2) can be written as

at $s=0$:

$$\begin{cases} I_{nm\eta} = \frac{1-\epsilon}{\pi} \int_{2\pi} I_{nm\eta} |\hat{n} \cdot \hat{s}| d\Omega & \text{for } n=1, \dots, N-1; \\ & m=1, \dots, M_n \text{ (gas scales)} \\ I_{s\eta} = \epsilon I_{b\eta w} + \frac{1-\epsilon}{\pi} \int_{2\pi} I_{s\eta} |\hat{n} \cdot \hat{s}| d\Omega & \text{for } n=s=N \text{ (soot scale)} \end{cases} \quad (8)$$

where the subscript s denotes the soot scale.

We now apply the FSK scheme [15] to each RTE. This process is demonstrated for the RTEs of each group of the gas scales. For the soot scale, i.e., the N -th scale ($n=s$), the same procedure needs to be followed for a scale with a single group, $M_s=1$. First, Eq. (6) is multiplied by Dirac's delta function $\delta(k_{nm} - \kappa_{nm\eta}(\underline{\phi}_0))$, followed by division with

$$f_{nm}(T_0, \underline{\phi}_0, k_{nm}) = \frac{1}{I_b(T_0)} \int_0^\infty I_{b\eta}(T_0) \delta(k_{nm} - \kappa_{nm\eta}(\underline{\phi}_0)) d\eta \quad (9)$$

where $\underline{\phi}_0$ and T_0 refer to a reference state, and k_{nm} is the reordered absorption coefficient variable of the nm -th group of a gas scale. The resulting equation is then integrated over the entire spectrum, leading to

$$\begin{aligned} \frac{dI_{nm\eta}}{ds} &= k_{nm} a_{nm} I_b - \lambda_{nm} I_{nm\eta} + \frac{\sigma_s}{4\pi} \int_{4\pi} I_{nm\eta}(\hat{s}') \Phi(\hat{s}, \hat{s}') d\Omega' \\ &\text{for } n=1, \dots, N-1; \quad m=1, \dots, M_n \\ &\text{for } n=s; \quad m=1(nm=s) \end{aligned} \quad (10)$$

where

$$I_{nm\eta} = \int_0^\infty I_{nm\eta} \delta(k_{nm} - \kappa_{nm\eta}(\underline{\phi}_0)) d\eta / f_{nm}(T_0, \underline{\phi}_0, k_{nm}) \quad (11)$$

The cumulative k -distribution g is the nondimensional spectral variable of the reordered spectrum, and for the m -th group of the n -th scale [8]

$$g_{nm} = \int_0^{k_{nm}} f_{nm}(T_0, \underline{\phi}_0, k) dk \quad (12)$$

a_m is the stretching factor for the m -th group of the n -th scale [8], and is calculated from

$$a_{nm} = \frac{f_{nm}(T, \underline{\phi}_0, k_{nm})}{f_{nm}(T_0, \underline{\phi}_0, k_{nm})} \quad (13)$$

and, finally, λ_{nm} is the overlap parameter of the m -th group of the n -th scale [8] with all other scales, and can be written as

$$\begin{aligned} \lambda_{nm} I_{nm\eta} &= k_{nm} I_{nm\eta} \\ &+ \frac{\int_0^\infty (\sum_{l \neq n} \sum_{q=1}^{M_l} \kappa_{lq\eta}(\underline{\phi})) I_{lq\eta} \delta(k_{nm} - \kappa_{nm\eta}(\underline{\phi}_0)) d\eta}{f_{nm}(T_0, \underline{\phi}_0, k_{nm})} \end{aligned} \quad (14)$$

Similarly, FSK reordering is performed on the boundary condition(s) with respect to $\kappa_{nm\eta}(\underline{\phi}_0)$ for each group of the gas scales, and $\kappa_{s\eta}(\underline{\phi}_0)$ for the soot scale, which results in

at $s=0$:

$$\begin{cases} I_{nm\eta} = \frac{1-\epsilon}{\pi} \int_{2\pi} I_{nm\eta} |\hat{n} \cdot \hat{s}| d\Omega & \text{for } n=1, \dots, N-1; \\ & m=1, \dots, M_n \\ I_{sg} = \epsilon a_w I_{bw} + \frac{1-\epsilon}{\pi} \int_{2\pi} I_{sg} |\hat{n} \cdot \hat{s}| d\Omega & \text{for } n=s=N \end{cases} \quad (15)$$

where a_w is the stretching factor for wall emission defined as

$$a_w = \frac{f_s(T_w, \underline{\phi}_0, k_s)}{f_s(T_0, \underline{\phi}_0, k_s)} \quad (16)$$

T_w is the wall temperature, which may be different from the medium temperature T .

Finally, the total radiative intensity is found by integrating each group over spectral space g , followed by summing over all groups and scales as

$$I = \sum_{n=1}^N \sum_{m=1}^{M_n} I_{nm} = \sum_{n=1}^N \sum_{m=1}^{M_n} \int_{g_{\min}}^1 I_{nm\eta} dg_{nm} \quad (17)$$

The second term on the right hand side of Eq. (10) is due to the overlap of the absorption coefficient of the m -th group of the n -th scale $\kappa_{nm\eta}$ with those of all other scales, which occurs over a part of the spectrum. The overlap parameter is a function of the state variables, as well as of the k - g distributions. Here we follow the approximate approach for overlap parameter calculations, as was done in the modified MSFSK method for gas-soot mixtures, assuming that the intensity emanating from a homogeneous nonscattering layer bounded by black walls is predicted exactly [9].

In Eq. (10), the reordering is performed in terms of absorption coefficients $\kappa_{nm\eta}$ and the interaction between $\kappa_{nm\eta}$ and κ_η during the reordering process is lumped into the overlap parameter λ_{nm} . The reordering can also be performed in terms of κ_η which, for a nonscattering homogeneous layer at temperature T , and bounded by a black wall at temperature T_w , leads to

$$\frac{dI_{nm\eta}^*}{ds} = \frac{k_{nm}^* I_b}{f(T, \underline{\phi}, k)} - k I_{nm\eta}^* \begin{cases} \text{for } n=1, \dots, N-1; \quad m=1, \dots, M_n \\ \text{for } n=s; \quad m=1(nm=s) \end{cases} \quad (18)$$

where

$$f(T, \underline{\phi}, k) = \frac{1}{I_b(T)} \int_0^\infty I_{b\eta}(T) \delta(k - \kappa_\eta(\underline{\phi})) d\eta \quad (19)$$

$$I_{nm\eta}^* = \int_0^\infty I_{nm\eta} \delta(k - \kappa_\eta(\underline{\phi})) d\eta / f(T, \underline{\phi}, k) \quad (20)$$

$$k_{nm}^* = \frac{1}{I_b} \int_0^\infty I_{b\eta}(T) \kappa_{nm\eta} \delta(k - \kappa_\eta(\underline{\phi})) d\eta \quad (21)$$

Reordering the boundary condition(s) with respect to $\kappa_\eta(\underline{\phi})$ leads to

at $s = 0$:

$$\begin{cases} I_{nm}^* = \frac{1 - \epsilon}{\pi} \int_{2\pi} I_{nm}^* |\hat{n} \cdot \hat{s}| d\Omega & \text{for } n = 1, \dots, N-1; \\ & m = 1, \dots, M_n \\ I_{sg}^* = \epsilon \frac{f(T_w, \phi, k)}{f(T, \phi, k)} I_{bw} + \frac{1 - \epsilon}{\pi} \int_{2\pi} I_{sg}^* |\hat{n} \cdot \hat{s}| d\Omega & \text{for } n = s = N \end{cases} \quad (22)$$

The solutions to Eqs. (10), (15), (18), and (22) for a homogeneous layer at temperature T bounded by black walls can be obtained analytically, and the total exiting intensities from each group of the gas scales from a layer of thickness L are

$$\begin{aligned} I_{nm} &= \int_0^1 I_{nm} dg \\ &= \int_0^\infty \frac{k_{nm}}{\lambda_{nm}} I_b [1 - \exp(-\lambda_{nm}L)] f_{nm}(T, \phi, k_{nm}) dk_{nm} \\ &\text{for } n = 1, \dots, N-1; \quad m = 1, \dots, M_n \end{aligned} \quad (23)$$

and

$$\begin{aligned} I_{nm}^* &= \int_0^1 I_{nm}^* dg = \int_0^\infty \frac{k_{nm}^*}{k} I_b [1 - \exp(-kL)] dk, \\ &\text{for } n = 1, \dots, N-1; \quad m = 1, \dots, M_n \end{aligned} \quad (24)$$

respectively. Since wall emission is added to the soot scale, the total exiting intensity from the soot scale from a layer of thickness L is

$$\begin{aligned} I_s &= \int_0^1 I_{sg} dg = \int_0^\infty a_w I_{bw} \exp(-\lambda_s L) f_s(T, \phi, k_s) dk_s \\ &+ \int_0^\infty \frac{k_s}{\lambda_s} I_b [1 - \exp(-\lambda_s L)] f_s(T, \phi, k_s) dk_s = I_{s1} + I_{s2} \end{aligned} \quad (25)$$

where I_{s1} is shorthand for the first term (wall emission), and I_{s2} for the second term (medium emission), and

$$\begin{aligned} I_s^* &= \int_0^1 I_{sg}^* dg = \int_0^\infty I_{bw} f(T_w, \phi, k) \exp(-kL) dk \\ &+ \int_0^\infty \frac{k^*}{k} I_b [1 - \exp(-kL)] dk = I_{s1}^* + I_{s2}^* \end{aligned} \quad (26)$$

where, again, I_{s1}^* (wall emission) and I_{s2}^* (medium emission) abbreviates the first and second term, respectively.

The spectrally integrated intensity I_{nm} should be equal to I_{nm}^* (for each group of the gas scales), and I_s should be equal to I_s^* (for the soot scale). For the m -th group of the n -th gas scale, this requirement leads to

$$\lambda_{nm} = k \quad \text{and} \quad k_{nm} f_{nm}(T, \phi, k_{nm}) dk_{nm} = k_{nm}^*(k) dk \quad (27)$$

Equation (27) provides the relationship between λ_{nm} and k_{nm} that is required to solve Eq. (10). One convenient way of determining λ_{nm} is using the relationship [5]

$$\int_0^{k_{nm}} k_{nm} f_{nm}(T, \phi, k_{nm}) dk_{nm} = \int_0^{k=\lambda_{nm}} k_{nm}^*(k) dk \quad (28)$$

For the soot scale, we use the strategy that the overlap parameter λ_s is determined by equating medium emission I_{s2} and I_{s2}^* , as was done in the modified MSFSK formulation [9]. To equate the overall intensity for the soot scale, the wall emissions I_{s1} and I_{s1}^* must

also be equal. The expression for I_{s1}^* is rearranged, employing the approximation for λ_s , as

$$I_{s1}^* = \int_0^\infty \frac{f(T_w, \phi, \lambda_s)}{k_s^*(T, \phi, \lambda_s)} k_s I_{bw} \exp(-\lambda_s L) f_s(T, \phi, k_s) dk_s \quad (29)$$

By comparison with the expression for I_{s1} in Eq. (24), it is clear that if

$$a_w(k_s) = \frac{f(T_w, \phi, \lambda_s)}{k_s^*(T, \phi, \lambda_s)} k_s, \quad \lambda_s = \lambda_s(k_s) \quad (30)$$

then I_{s1} is equal to I_{s1}^* .

3 Evaluation of Overlap Parameter

For efficient calculations, the overlap parameter needs to be available from a database of narrow band multigroup (NBMG) k -distributions for individual gas species. The advantages of using NBMG k -distributions are: (1) groups within each narrow band are scalable, and hence can be combined to obtain coarser k - g distributions; (2) the use of NBMG k -distributions of individual gas species allows the inclusion of nongray absorbing particles in the participating medium [4]; (3) mixing of k - g distributions is more accurate when performed at the narrow band level, as compared with the full-spectrum level; and (4) since the wavenumbers within a narrow band are grouped according to their temperature dependence, NBMG k -distributions can be used to construct full-spectrum multigroup k - g distributions, which are known to be more accurate for temperature inhomogeneities in multiphase mixtures.

For the m -th group of the n -th gas scale, substituting Eq. (21), the right hand side (RHS) of Eq. (28) may be rewritten in terms of a narrow band-based k_{nm}^*

$$\begin{aligned} \text{RHS} &= \sum_{i=1}^{N_{nb}} \frac{I_{bi}}{I_b} \int_0^{k=\lambda_{nm}} k_{nm,i}^*(k) dk \\ &= \int_0^{k=\lambda_{nm}} \sum_{i=1}^{N_{nb}} \frac{I_{bi}}{I_b} \frac{1}{\Delta \eta} \int_{\Delta \eta} \kappa_{nm\eta} \delta(k - \kappa_\eta) d\eta dk \end{aligned} \quad (31)$$

where $k_{nm,i}^*$ is the narrow band counterpart of k_{nm}^* , N_{nb} is the number of narrow bands comprising the entire spectrum, and the narrow band integrated Planck function I_{bi} is defined as

$$I_{bi} = \int_{\Delta \eta_i} I_{b\eta} d\eta \quad (32)$$

As always, in the narrow band-based k -distribution approach, we have assumed that $I_{b\eta}$ is constant over $\Delta \eta_i$ and can be approximated by $I_{bi}/\Delta \eta_i$.

In order to evaluate the integrals involving $k_{nm,i}^*$ in Eq. (31) in terms of NBMG k -distributions, we consider the quantity Q_{nm} as

$$Q_{nm} = \frac{1}{\Delta \eta} \int_{\Delta \eta} \kappa_{nm\eta} \exp(-\kappa_\eta L) d\eta \quad (33)$$

for the i -th narrow band. Physically, Q_{nm} is related to emission from the m -th group of the n -th scale for the given narrow band i , attenuated over path L by the entire gas mixture. Q_{nm} can be rewritten as

$$\begin{aligned} Q_{nm} &= \frac{1}{\Delta \eta} \int_{\Delta \eta} \kappa_{nm\eta} \int_0^\infty \exp(-kL) \delta(k - \kappa_\eta) dk d\eta \\ &= \int_0^\infty k_{nm,i}^* \exp(-kL) dk = \mathcal{L}(k_{nm,i}^*) \end{aligned} \quad (34)$$

i.e., Q_{nm} is the Laplace transform of $k_{nm,i}^*$.

Previously, in the modified MSFSK development [9], it was shown that, (1) on a narrow band basis, the spectral behavior of different species is essentially statistically uncorrelated, and (2) the soot absorption coefficient is approximately constant across each narrow band [4,7,9]. Since the wavenumbers within a narrow band are placed into exclusive spectral groups, the assumption of statistical uncorrelatedness in spectral behavior between a group (within a narrow band) of one gas species and the narrow band of another gas species still holds. With this assumption, Q_{nm} can be written as (after applying the k -distribution method [9])

$$Q_{nm} \approx \int_{g_{nm,i}=0}^1 \prod_{l \neq s,n}^N \left(\int_{g_{l,i}=0}^1 k_{nm,i} \exp\left(-\sum_{l \neq s,n} k_{l,i}L - k_{nm,i}L - \bar{k}_{s,i}L\right) dg_{l,i} \right) dg_{nm,i} \quad (35)$$

where $\bar{k}_{s,i}$ is the narrow band average value of the soot absorption coefficient.

Equating Eqs. (34) and (35), we have

$$\mathcal{L}(k_{nm,i}^*) \approx \int_{g_{nm,i}=0}^1 \prod_{l \neq s,n}^N \left(\int_{g_{l,i}=0}^1 k_{nm,i} \exp\left(-\sum_{l \neq s,n} k_{l,i}L - k_{nm,i}L - \bar{k}_{s,i}L\right) dg_{l,i} \right) dg_{nm,i} \quad (36)$$

Using the integral property of the Laplace transform and then taking the inverse, we obtain

$$\int_0^{k=\lambda_{nm}} k_{nm,i}^*(k) dk \approx \int_{g_{nm,i}=0}^1 \prod_{l \neq s,n}^N \left(\int_{g_{l,i}=0}^1 k_{nm,i} H\left(\lambda_{nm} - \sum_{l \neq s,n} k_{l,i} - k_{nm,i} - \bar{k}_{s,i}\right) dg_{l,i} \right) dg_{nm,i} \quad (37)$$

where H is the Heaviside step function.

The LHS of Eq. (28) is also readily expressed in terms of narrow band k -distributions for the m -th group of n -th gas scale as

$$\begin{aligned} \text{LHS} &= \int_0^{k_{nm}} k_{nm} \frac{1}{I_b} \int_0^\infty I_{b\eta} \delta(k_{nm} - \kappa_{nm\eta}) d\eta dk_{nm} \\ &= \sum_{i=1}^{N_{nb}} \frac{I_{bi}}{I_b} \int_0^{k_{nm}} k_{nm} \frac{1}{\Delta\eta_i} \int_{\Delta\eta_i} \delta(k_{nm} - \kappa_{nm\eta}) d\eta dk_{nm} \\ &= \sum_{i=1}^{N_{nb}} \frac{I_{bi}}{I_b} \int_0^{g_{nm,i}(k_{nm})} k_{nm,i} dg_{nm,i} \end{aligned} \quad (38)$$

Equating the LHS and RHS, we obtain a generic expression for the determination of the overlap parameter λ_{nm} of the m -th group of the n -th gas scale, based on NB k -distributions of individual gas species as

$$\begin{aligned} &\sum_{i=1}^{N_{nb}} \frac{I_{bi}}{I_b} \int_0^{g_{nm,i}(k_{nm})} k_{nm,i} dg_{nm,i} \\ &= \sum_{i=1}^{N_{nb}} \frac{I_{bi}}{I_b} \int_0^1 \prod_{g_{nm,i}=0}^N \left(\int_{g_{l,i}=0}^1 k_{nm,i} H\left(\lambda_{nm} - \sum_{l \neq s,n} k_{l,i} - k_{nm,i} - \bar{k}_{s,i}\right) dg_{l,i} \right) dg_{nm,i}; \quad \text{for } \begin{matrix} n = 1, \dots, N-1, \\ m = 1, \dots, M_n(\text{gas scales}) \end{matrix} \end{aligned} \quad (39)$$

The integrals in Eq. (39) can be evaluated efficiently, based on the NBMG database, as outlined by Wang and Modest [7]. The overlap parameter for soot, being treated as a single-group scale, can

be obtained from the modified MSFSK formulation of Pal and Modest [9].

4 Evaluation of Modified Wall Stretching Factor

Incorporation of wall emission into the soot scale, Eq. (15), introduces the wall stretching factor a_w [9]. It was demonstrated by Pal and Modest [9] that MSFSK calculations using the modified a_w from Eq. (30) are more accurate, as compared with calculations using the direct a_w from Eq. (16), because only the modified a_w recovers the LBL results for homogeneous media with arbitrary boundary wall temperatures. For the calculation of the modified a_w in the present narrow band-based hybrid method, the same approach was considered as outlined in the modified MSFSK formulations [9].

5 NBMG Database Construction

Accurate and compact databases of NBMG k -distributions are constructed as part of this work. The spectral absorption coefficients for water vapor are calculated from HITEMP 2000, and for carbon dioxide from CSDS-1000. The resulting NBMG k - g distributions of the combustion gases are stored for various values of total pressure, local gas temperature, and species mole fraction, as described in Ref. [13], but now for four groups.

The wavenumbers within each narrow band of the gas species in 0.01 cm^{-1} intervals are placed into four exclusive spectral groups according to the temperature dependence of the absorption coefficients. Details of the grouping of wavenumbers can be obtained from Ref. [8]. Once all spectral locations are grouped, the narrow band k - g distributions are calculated for each group and each gas species. Details of the k - g distribution construction can be obtained from Ref. [13]. After the calculation of the initial k -distributions, data compaction is performed using a Gaussian quadrature scheme with fixed g -values, as outlined by Wang and Modest [13].

To obtain the k -distribution for an arbitrary state, interpolation is needed between precalculated states stored in the database. For a single gas species, the k -distribution is specified by total pressure (P), local gas temperature (T), and mole fraction (x). Hence, three-dimensional interpolation in (P, T, x) is required. In order to achieve acceptable accuracy with small computational cost, a 1D spline interpolation is used for T , and bilinear interpolation for P - x [13].

The newly constructed NBMG database is scalable, i.e., for faster computation, the groups can be combined to obtain coarser groups, both at the narrow band and full-spectrum level. The narrow band k - g distributions of the combined group n from finer groups m can be calculated [6,8] as

$$1 - g_{n,i}(k) = \sum_m (1 - g_{m,i}(k)) \quad (40)$$

where $g_{n,i}$ and $g_{m,i}$ are the cumulative k -distributions of the i -th narrow band for the same k -values of the combined groups and original groups, respectively [6].

6 Sample Calculations

6.1 1D Problem. Sample calculations were performed for a 1D medium, containing emitting-absorbing CO_2 - H_2O - N_2 gas mixtures, as well as soot, confined between cold black walls. The mixture consists of two different homogeneous layers (denoted as left and right layers/column) adjacent to each other at a total pressure of 1 bar. The left layer has a fixed width of 50 cm. The width of the right layer was varied in the calculations. The radiative heat flux leaving from the right layer (i.e., radiative flux at the right wall) was calculated using the LBL method, the single-scale FSK method, the modified MSFSK method, and the present narrow band-based MSMGFSK method (using two and four groups).

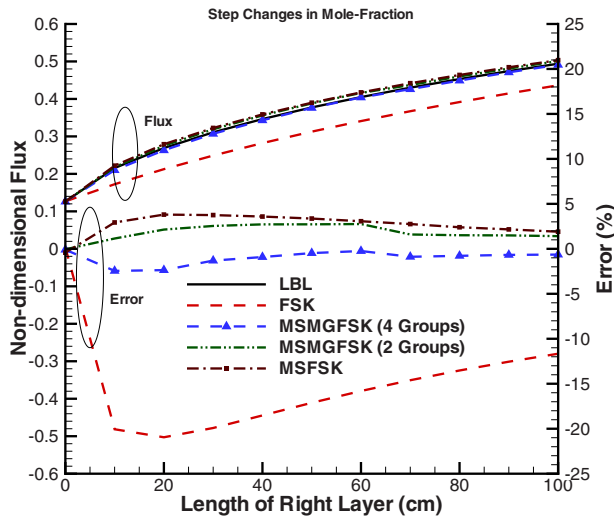


Fig. 1 Nondimensional heat flux leaving an inhomogeneous slab at a total pressure of 1 bar with step changes in mole fraction: The left layer contains 20% CO₂, 2% H₂O, and no soot, and the right layer contains 2% CO₂, 20% H₂O, and 0.1 ppm soot; both layers are at a constant temperature of 1000 K

For all LBL calculations, absorption coefficients of CO₂ and H₂O were obtained from the CDSD-1000 and the HITEMP spectroscopic databases, respectively, and for the *k*-distribution based calculations, the *k*-*g* data for CO₂ and H₂O from the new narrow band multigroup databases. Soot absorption coefficients were evaluated, invoking the assumption of small particles (scattering from the agglomerated soot particles was ignored for all sample calculations) with the complex index of refraction given by Chang and Charalampopoulos [16].

Figure 1 shows the results for the case of a gas-soot mixture with mole fraction step changes in all three scales: CO₂, H₂O, and soot. The left layer contains 20% CO₂, 2% H₂O, and no soot, while the right layer contains 2% CO₂, 20% H₂O, and 0.1 ppm soot. Both layers are at a constant temperature of 1000 K. In this inhomogeneous problem, the error of the basic single-scale FSK method reaches more than 20%. In comparison to that, if the gas-soot mixture is broken up into several scales, one for each species, the modified MSFSK method produces considerably more accurate solutions, with a maximum error below 4%. The narrow band-based MSMGFSK calculations were performed using two or four groups for each gas scale, and soot was considered as a single-group scale. Both the two and four groups based MSMGFSK calculations result in slightly better accuracy (maximum error limited to less than 3%) compared with the modified MSFSK method.

Figure 2 shows the results for the case of a gas-soot mixture with step changes in temperature. Both layers contain 20% CO₂, 20% H₂O, and 0.1 ppm soot. The left layer is at 1500 K, while the right layer is at 500 K. In this case, the maximum error of the basic single-scale FSK method reaches 9%. The modified MSFSK method reduces the maximum error to below 5%. Both the two and four groups based MSMGFSK calculations still yield better accuracy (maximum error limited to 2% for both). It is observed that the accuracy of the two and four groups based calculations are close to each other, which apparently is due to the presence of compensating errors between grouping of absorption coefficients and mixing among different absorbing species.

Radiative transfer calculations were also performed for the case of a gas-soot mixture with mole fraction step changes in all the three scales (two gas species and soot) in addition to a step change in temperature, and results are shown in Fig. 3. The left hot layer contains 20% CO₂, 2% H₂O, and no soot; the right cold layer has

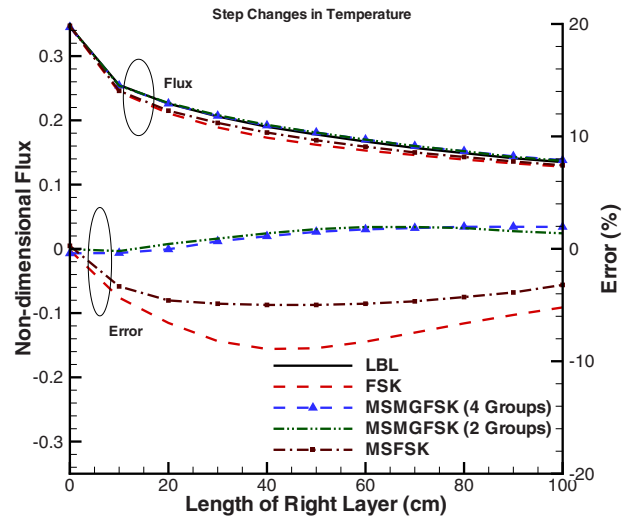


Fig. 2 Nondimensional heat flux leaving an inhomogeneous slab at a total pressure of 1 bar with step changes in temperature: left layer at 1500 K, and right layer at 500 K; both layers contain 20% CO₂, 20% H₂O, and 0.1 ppm soot

0.1 ppm of soot with the gas compositions reversed. It is observed here that the two and four group-based MSMGFSK method have a maximum error of only 5% for very high optical thickness, whereas the single-scale FSK method incurs a maximum error close to 60%. The modified MSFSK method incurs a maximum error of 40%, demonstrating its inability to handle strong temperature inhomogeneities in multiphase mixtures. In all cases, it is seen that the two group-based calculations result in excellent accuracy, and only 2*N* RTEs need to be solved (with *N* as the number of species/scales).

6.2 2D Problem. Next we consider a two-dimensional axisymmetric ethylene-air jet flame numerically studied by Mehta [17]. This flame simulates the jet flame experimentally studied by Kent and Honnery [18]. The burner of this Kent and Honnery flame (KH87) consists of a cylindrical nozzle of diameter $d_j = 3$ mm. The Reynolds number varies from 7500 to 15,000. A three-dimensional wedge-like (wedge angle of 10 deg) grid system was employed to simulate the axisymmetric flame by applying periodic boundary conditions on the sides. The dimensions in the *x*- and *z*-directions are $30d_j$ and $250d_j$, respectively. The details of modeling the KH87 flame can be found elsewhere [17]. The converged results of that study were used as a frozen data field for radiation calculations. CO₂, H₂O, CO, and soot are the major products of combustion, and hence, are considered in radiation calculations in addition to ethylene (fuel). The concentrations of the major species and the temperature data are shown in Fig. 4. The pressure is uniform (equal to 1 bar). The local radiative heat source term is calculated using the LBL, the basic single-scale FSK, the modified MSFSK, and the two and four group narrow band-based MSMGFSK approaches, employing the P-1 method as the RTE solver. Relative errors are determined by comparison with LBL as

$$\text{error}(\%) = \frac{\nabla \cdot q_{\text{LBL}} - \nabla \cdot q_{\text{FSK/MSFSK/MSMGFSK}}}{\nabla \cdot q_{\text{LBL,max}}} \times 100 \quad (41)$$

For 2D LBL calculations, the absorption coefficients of C₂H₄ and CO were obtained from the HITRAN-2004 [19] and HITEMP [20] spectroscopic databases, respectively. Narrow band single-group databases of *k*-*g* distributions were compiled for gas species such as C₂H₄ and CO, as outlined by Wang and Modest [13], and were used for 2D calculations. The total number of RTEs solved in each method for the 2D problem is: 1.5 million for LBL, 10 for

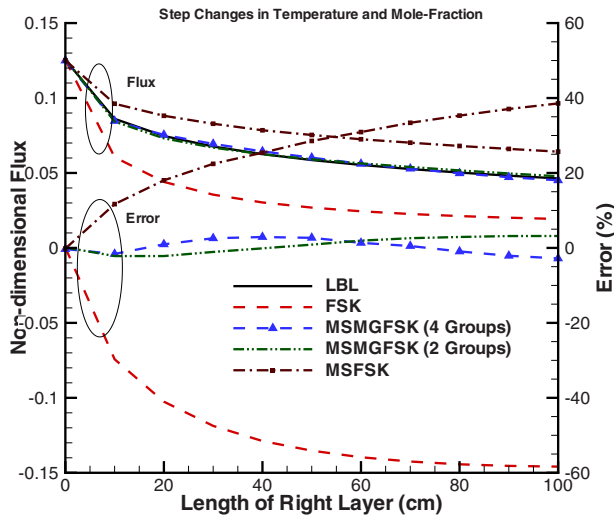


Fig. 3 Nondimensional heat flux leaving an inhomogeneous slab at a total pressure of 1 bar with step changes in temperature and mole fraction: The hot left layer contains 20% CO₂, 2% H₂O, and no soot at 1500 K, and the cold right layer contains 2% CO₂, 20% H₂O, and 0.1 ppm soot at 500 K

single-scale FSK, 4×10 for modified MSFSK (CO₂ and H₂O as combined scale, each other species as one scale), and 7×10 and 11×10 for narrow band-based MSMGFSK (each species as one scale, CO₂ and H₂O scales having two and four groups each, respectively), where 10 is the number of quadrature points.

The local radiative heat source term calculated using the LBL method is shown in Fig. 5(a). Figure 5(b) shows that the single-scale FSK method generates large errors for gas-soot mixtures with varying ratios of concentrations (the maximum error in the present problem reaches as much as 35% near the inlet). In the multiscale approach, CO₂ and H₂O are combined into a single scale since they have approximately the same ratio of concentration throughout the combustion chamber, while C₂H₄, CO, and soot are treated as single-group individual scales. Mixing of CO₂ and H₂O is performed with their local concentrations using the narrow band-based *k*-distribution mixing rule [4]. The maximum error is now limited to 7% near the inlet (region of high errors), as seen in Fig. 5(c). Figure 5(d) shows the errors incurred in the two group narrow band-based MSMGFSK calculations. In this approach, the C₂H₄, CO, and soot are treated as single-group scales, while CO₂ and H₂O are treated as two separate scales, each having two spectral groups. The maximum error for this case is limited to 4%. The results from the four group-based MSMGFSK methods are approximately the same as the two group case and, hence, are not shown here. This is a substantial improvement, and the accuracy of the new narrow band-based MSMGFSK approach

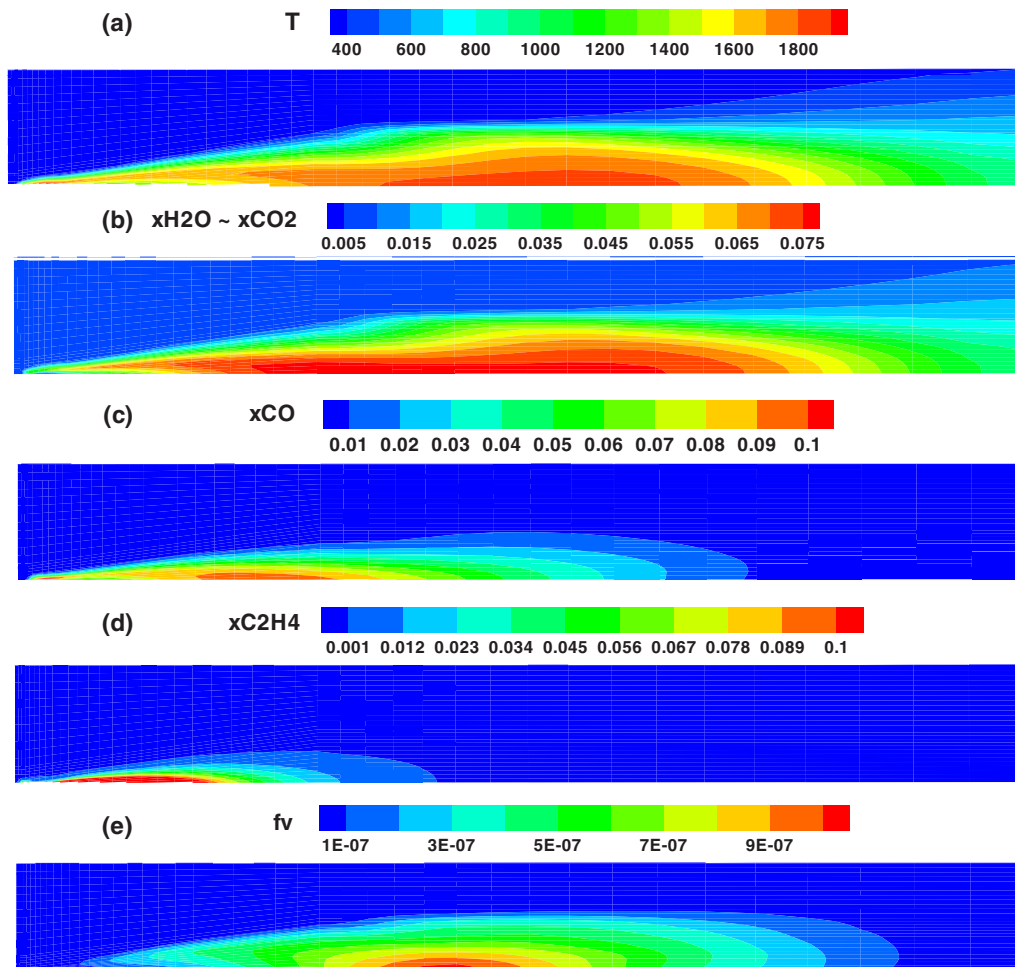


Fig. 4 Temperature and mole fraction distributions in numerically simulated KH87 flame, (a) temperature distribution, (b) mole fraction distribution of H₂O and approximately CO₂ (wherever there is little CO), (c) mole fraction distribution of CO, (d) mole fraction distribution of C₂H₄, and (e) distribution of soot volume fraction

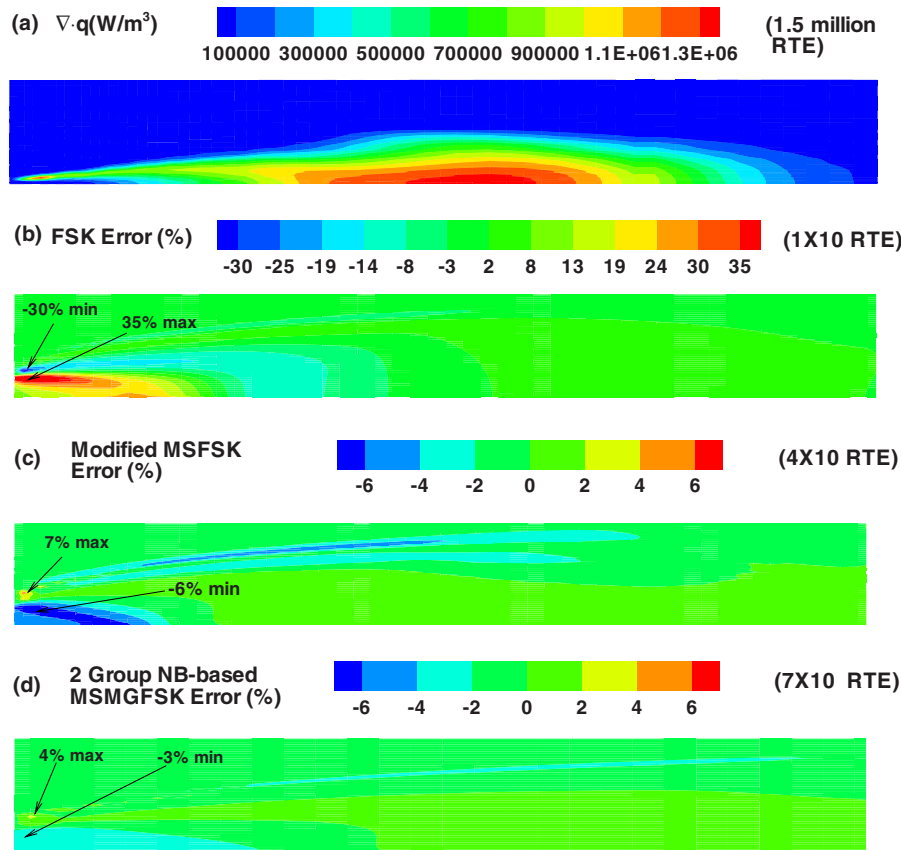


Fig. 5 (a) Local radiative heat source using LBL method and relative error (compared with LBL) for heat source calculations using (b) the single-scale FSK method, (c) the modified MSFSK method, and (d) the two group narrow band-based MSMGFSK method

for gas-soot mixtures is clearly demonstrated. CPU time for the LBL calculations is approximately 56 h on a 2.4 GHz AMD Opteron machine, while the single-scale FSK, the modified MSFSK, the two group-based MSMGFSK, and the four group-based MSMGFSK take only 7 s, 41 s, 78 s, and 110 s (i.e., typical times required for chemistry calculations in a combustion problem), respectively, for this calculation. This implies factors of 3×10^4 , 5×10^3 , 2.5×10^3 , and 2×10^3 CPU time improvement, respectively, over LBL cost.

7 Conclusion

In this paper, a new narrow band-based multiscale multigroup full-spectrum k -distribution method has been developed for radiation calculations involving nongray gas-soot mixtures with gray wall emission. This spectral method is capable of producing close-to-LBL accuracy for radiation calculations in general combustion problems with multiphase mixtures, temperatures, and concentration inhomogeneities. Accurate and compact narrow band multigroup databases were constructed for the most important combustion gases: CO_2 and H_2O . Sample calculations were performed for both 1D media and for a 2D ethylene-air jet flame with gas-soot mixtures. The narrow band-based hybrid method is more accurate than the single-scale FSK method for all the cases, and more accurate than the modified MSFSK method for cases with temperature inhomogeneity. It is observed that the two group-based calculations produce similar accuracy as the four group-based calculations, both yielding close-to-LBL accuracy, but requiring less computational time. In realistic combustion problems, the narrow band-based multiscale multigroup method is able to provide very accurate results (an order of magnitude more accurate than the FSK, and with several orders of magnitude lesser computational cost than LBL).

References

- [1] Denison, M. K., and Webb, B. W., 1993, "A Spectral Line Based Weighted-Sum-of-Gray-Gases Model for Arbitrary RTE Solvers," *ASME J. Heat Transfer*, **115**, pp. 1004–1012.
- [2] Pierrot, L., Rivière, Ph., Soufiani, A., and Taine, J., 1999, "A Fictitious-Gas-Based Absorption Distribution Function Global Model for Radiative Transfer in Hot Gases," *J. Quant. Spectrosc. Radiat. Transf.*, **62**, pp. 609–624.
- [3] Modest, M. F., and Zhang, H., 2002, "The Full-Spectrum Correlated- k Distribution for Thermal Radiation From Molecular Gas-Particulate Mixtures," *ASME J. Heat Transfer*, **124**(1), pp. 30–38.
- [4] Modest, M. F., and Riazzi, R. J., 2005, "Assembly of Full-Spectrum k -Distributions From a Narrow-Band Database; Effects of Mixing Gases, Gases and Nongray Absorbing Particles, and Mixtures With Nongray Scatterers in Nongray Enclosures," *J. Quant. Spectrosc. Radiat. Transf.*, **90**(2), pp. 169–189.
- [5] Zhang, H., and Modest, M. F., 2002, "A Multi-Scale Full-Spectrum Correlated- k Distribution for Radiative Heat Transfer in Inhomogeneous Gas Mixtures," *J. Quant. Spectrosc. Radiat. Transf.*, **73**(2–5), pp. 349–360.
- [6] Zhang, H., and Modest, M. F., 2003, "Scalable Multi-Group Full-Spectrum Correlated- k Distributions for Radiative Heat Transfer," *ASME J. Heat Transfer*, **125**(3), pp. 454–461.
- [7] Wang, L., and Modest, M. F., 2005, "Narrow-Band Based Multi-Scale Full-Spectrum k -Distribution Method for Radiative Transfer in Inhomogeneous Gas Mixtures," *ASME J. Heat Transfer*, **127**, pp. 740–748.
- [8] Pal, G., Modest, M. F., and Wang, L., 2008, "Hybrid Full-Spectrum Correlated k -Distribution Method for Radiative Transfer in Strongly Nonhomogeneous Gas Mixtures," *ASME J. Heat Transfer*, **130**, pp. 082701–082708.
- [9] Pal, G. and Modest, M. F., 2009, "A Multi-Scale Full-Spectrum k -Distribution Method for Radiative Transfer in Nonhomogeneous Gas-Soot Mixture With Wall Emission," *Comp. Therm. Sci.*, **1**(2), pp. 137–158.
- [10] Wang, L., Haworth, D. C., Turns, S. R., and Modest, M. F., 2005, "Interactions Among Soot, Thermal Radiation, and NOx Emissions in Oxygen-Enriched Turbulent Nonpremixed Flames: A CFD Modeling Study," *Combust. Flame*, **141**(1–2), pp. 170–179.
- [11] Solovjov, V., and Webb, B. W., 2001, "An Efficient Method of Modeling Radiative Transfer in Multicomponent Gas Mixtures With Soot," *ASME J. Heat Transfer*, **123**, pp. 450–457.
- [12] Wang, L., Modest, M. F., Haworth, D. C., and Turns, S. R., 2005, "Modeling Nongray Soot and Gas-Phase Radiation in Luminous Turbulent Nonpremixed

- Jet Flames,” *Combust. Theory Modell.*, **9**(3), pp. 479–498.
- [13] Wang, A., and Modest, M. F., 2005, “High-Accuracy, Compact Database of Narrow-Band k -Distributions for Water Vapor and Carbon Dioxide,” *J. Quant. Spectrosc. Radiat. Transf.*, **93**, pp. 245–261.
- [14] Modest, M. F., 2003, *Radiative Heat Transfer*, 2nd ed., Academic, New York.
- [15] Modest, M. F., 2003, “Narrow-Band and Full-Spectrum k -Distributions for Radiative Heat Transfer—Correlated- k vs. Scaling Approximation,” *J. Quant. Spectrosc. Radiat. Transf.*, **76**(1), pp. 69–83.
- [16] Chang, H., and Charalampopoulos, T. T., 1990, “Determination of the Wavelength Dependence of Refractive Indices of Flame Soot,” *Proc. R. Soc. London*, **430**(1880), pp. 577–591.
- [17] Mehta, R. S., 2008, “Detailed Modelling of Soot Formation and Turbulence-Radiation Interactions in Turbulent Jet Flames,” Ph.D. thesis, Pennsylvania State University, University Park, PA.
- [18] Kent, J. H., and Honnery, D., 1987, “Modeling Sooting Turbulent Jet Flames Using an Extended Flamelet Technique,” *Combust. Sci. Technol.*, **54**, pp. 383–397.
- [19] Rothman, L. S., Jacquemart, D., Barbe, A., Chris Benner, D., Birk, M., Brown, L. R., Carleer, M. R., Chackerian, C., Jr., Chance, K., Coudert, L. H., Dana, V., Devi, V. M., Flaud, J.-M., Gamache, R. R., Goldman, A., Hartmann, J.-M., Jucks, K. W., Maki, A. G., Mandin, J.-Y., Massie, S. T., Orphal, J., Perrin, A., Rinsland, C. P., Smith, M. A. H., Tennyson, J., Tolchenov, R. N., Toth, R. A., Vander Auwera, J., Varanasi, P., and Wagner, G., 2005, “The HITRAN 2004 molecular spectroscopic database,” *J. Quant. Spectrosc. Radiat. Transf.*, **96**, pp. 139–204.
- [20] Rothman, L. S., Watson, R. B., Gamache, R., Schroeder, J. W., and McCann, A., and 1995, “HITRAN, HAWKS and HITEMP: High-Temperature Molecular Database,” *Proc. SPIE*, **2471**, pp. 105–111.